ELSEVIER

New representatives of the linear structure series containing empty Ga/Ge cubes in the Sm–Ga–Ge system

Yaroslav O. Tokaychuk[a],[*], Yaroslav E. Filinchuk[a],[1], Anatoliy O. Fedorchuk[b], Artem Yu. Kozlov[c], Ivanna R. Mokra[b]

[a]*Laboratory of Crystallography, University of Geneva, 24 quai Ernest-Ansermet, CH-1211 Geneva, Switzerland*
[b]*Department of Inorganic Chemistry, Ivan Franko National University of Lviv, Kyryla i Mefodiya str. 6, UA-79005 Lviv, Ukraine*
[c]*Institute of Metallurgy, Clausthal University of Technology, Robert-Koch-Str. 42, D-38678 Clausthal-Zellerfeld, Germany*

Dedicated to the memory of Prof. Oksana Bodak

Abstract

New ternary intermetallic compounds $Sm_2Ga_{7-x}Ge_x$ ($x = 5.2-6.1$) and $Sm_4Ga_{11-x}Ge_x$ ($x = 5.76-8.75$) were synthesized and their crystal structures were determined by X-ray powder diffraction at compositions $Sm_2Ga_{1.8}Ge_{5.2}$ and $Sm_4Ga_{5.24}Ge_{5.76}$. $Sm_2Ga_{1.8}Ge_{5.2}$ crystallizes with the $Ce_2(Ga_{0.1}Ge_{0.9})_7$ type of structure (space group $Cmce$, Pearson code $oS80$–8.00, $a = 8.46216(13)$, $b = 8.15343(13)$, $c = 21.1243(3)$ Å, $Z = 8$), while $Sm_4Ga_{5.24}Ge_{5.76}$ exhibits a new structure (space group $Cmmm$, Pearson code $oS52$–22.00, $a = 4.21038(4)$, $b = 35.8075(3)$, $c = 4.14023(4)$ Å, $Z = 2$). Both structures are the members of the linear intergrowth structure series built up from segments of $BaAl_4$, AlB_2 and α-Po structure types. Their Ga/Ge networks contain characteristic empty cubes with one side capped by an atom subjected to an intrinsic displacive disorder. A model of Ga/Ge localization was suggested on the basis of crystal-chemical analysis.
© 2006 Elsevier Inc. All rights reserved.

Keywords: Ternary gallides; Crystal structure; X-ray powder diffraction; Linear structure series; Disorder

1. Introduction

Gallium-rich intermetallic compounds reveal a variety of Ga frameworks, like two-dimensional graphite-like networks in the structures of AlB_2-type digallides, which become corrugated in the $CaIn_2$-type structures [1]. At higher Ga content ($CaGa_4$ [2] and $PuGa_6$ [3] structure types) the frameworks become three-dimensional. Characteristic Ga_8 cubes with two opposite faces caped by Ga atoms appear in hexagallides. In a pentagallide $YbGa_5$ a pronounced disorder of gallium atoms has been recently identified for similar bicapped Ga cubes [4]. It was suggested that the disorder appears due to a tendency of three-bonded Ga atoms to achieve the "optimum" distances and a four-bonded state. Gallium atoms in a five-bonded state tend to compensate this distortion, resulting in their intrinsic disorder and split atom positions.

Partial substitution of Ga by Ge, a fourth group element of similar atomic size, stabilizes a yet more diverse variety of crystal structures. A number of ternary compounds were reported in the rare earth–gallium–germanium and related systems [5,6]. Here we report on synthesis and structures of two novel ternary compounds in the Sm–Ga–Ge system. The Ga/Ge networks in these structures contain characteristic empty cubes with only one side capped, which similarly to $YbGa_5$ display an intrinsic displacive atomic disorder.

2. Experimental part

2.1. Sample preparation and elemental analysis

The alloys were prepared by arc-melting Sm (99.9%), Ga and Ge (each 99.99%) elements on a water-cooled copper

---

base under a purified argon atmosphere. We have used molten Ti as an oxygen getter to ensure removal of any oxygen trances in the argon atmosphere. To improve homogeneity, each sample was remelted three times. The ingots were wrapped into tantalum foil, annealed at 870 K in vacuum for 1 month and quenched in cold water. For 2 g alloys the mass losses during the melting did not exceed 1%. The samples for detailed structural study ($Sm_{22}Ga_{20}Ge_{58}$ and $Sm_{28}Ga_{35}Ge_{37}$) were examined for microstructure and composition by scanning electron microscopy and energy-dispersive X-ray microanalysis (SEM/EDX). The samples were ground, polished under alcohol and etched in a solution of 1 mL HNO_3/20 mL acetic acid/60 mL ethylene glycol/19 mL H_2O for 15 s at room temperature. Then samples were investigated with a Camscan 44-SEM (UK) equipped with an EDX detector. The results of the metallographic analysis of these samples are in a good agreement with their nominal compositions and results of X-ray diffraction (see Section 2.2). According to the EDX analysis, the composition of the main phase for the first sample is $Sm_{1.94}Ga_{1.74}Ge_{5.32}$ and $Sm_{4.07}Ga_{5.12}Ge_{5.80}$ for the second.

2.2. X-ray powder diffraction

X-ray powder diffraction patterns were obtained at room temperature on a Bruker D8 Advance diffractometer with $CuK_{\alpha1}$ radiation. The *FullProf*.2000 program package [7] was used in all calculations. The similarity of the Ga and Ge atomic scattering factors prevents their being distinguished by X-ray diffraction without recourse to measurements at synchrotron source by exploiting the resonant scattering contribution. In this work any Ga/Ge position was assumed to be occupied by a mixture of Ga and Ge atoms in a ratio given by the nominal composition. Such positions are referred to as "X".

The $Sm_2Ga_{1.8}Ge_{5.2}$ structure was refined by the Rietveld method starting from coordinates of the parent structure type $Ce_2(Ga_{0.1}Ge_{0.9})_7$ [8], in space group $Cmce$, which is a superstructure of the $SmNiGe_3$ structure type [9]. Selection of the doubled cell parameters a and b, compared to a $4 \times 4 \times 21$ Å subcell, was supported by the appearance of clear superstructure reflections. Refined isotropic atomic displacement parameters suggested a disorder in one of the six X positions. The disorder was modelled by replacing one $8f$ Wyckoff position with a half-occupied split $16g$ position. This improved considerably the fit and standard uncertainties of the structural parameters. The refined separation of the split atoms is 0.589(6) Å. In the final refinement cycles an overall isotropic displacement parameter was refined for the X positions. 11.2 wt% of Ge (space group $Fd\bar{3}m$, $a = 5.65807(11)$ Å) were additionally found in the $Sm_{22}Ga_{20}Ge_{58}$ sample. This secondary phase was modelled with one scale factor and one cell parameter, while the profile parameters were refined first and fixed in the final cycles of the refinement. Finally, 33 parameters were allowed to vary for both phases: sample shift, two

scale factors, four cell parameters, six profile parameters for the main phase (pseudo-Voigt profile), 17 positional parameters, two atomic displacements and one texture parameter. The background was defined using a Fourier filtering technique.

The $Sm_4Ga_{5.24}Ge_{5.76}$ structure was solved ab initio. The X-ray powder diffraction pattern was indexed by an orthorhombic cell with $a = 4.2101(2)$, $b = 35.807(2)$, $c = 4.1411(2)$ Å, using the DICVOL91 program [10]. There were no superstructure reflections indicating a possible doubling of the a and c parameters. Systematic absences suggested five possible space groups: $C222$, $Cnm2$, $Cm2m$, $C2mm$ and $Cmmm$. Profile parameters were derived from the Le Bail fit (FULLPROF.2000) and the structure was solved in space group $Cmmm$ by global optimization in direct space (program FOX [11]). The structure was refined by the Rietveld method. Similar to the $Sm_2Ga_{1.8}Ge_{5.2}$ structure, some X positions were identified as split: $X1$ ($2a$ site split to $16r$), $X2$ ($4g$ site split to $8q$) and $X3$ ($4k$ site split to $8n$), with occupancies 0.125, 0.5 and 0.5, respectively. The split atoms are separated by a distance of 0.588(18), 0.577(7) and 0.630(6) Å for $X1$, $X2$ and $X3$ positions, respectively. In the final refinement cycles an overall isotropic displacement parameter was refined for the three split X positions, while isotropic displacement parameters for the remaining atoms were refined independently. The displacement parameter for the $X4$ position is larger than those for the other X atoms. The $X4$ atom is influenced by the disorder of its first neighbour, $X1$. The pronounced disorder of the $X1$ site induces a small disorder of the $X4$ site. However, the latter has been satisfactory modelled by merely a higher displacement parameter. Two known ternary phases [12] have been identified as impurities: $SmGa_{1.1}Ge_{0.9}$ (1.3(1) wt%, structure type α-$ThSi_2$, space group $I4_1/amd$, $a = 4.18898(17)$, $c = 14.4687(9)$ Å) and $SmGa_{0.8}Ge_{2.2}$ (0.7(1) wt%, structure type $AuCu_3$, space group $Pm\bar{3}m$, $a = 4.33562(11)$ Å). For these phases only scale factors and cell parameters were included in the refinement, while their profile parameters were refined first and then fixed in the final refinement cycles. The background was defined using a Fourier filtering technique. In the final refinement cycles 31 parameters were allowed to vary: sample shift, three scale factors, six cell parameters, six profile parameters for the main phase (pseudo-Voigt profile), 12 positional parameters, six atomic displacement and one texture parameters.

The diffraction patterns for the $Sm_{22}Ga_{20}Ge_{58}$ and $Sm_{28}Ga_{35}Ge_{37}$ samples are presented in Fig. 1. Crystal data and details of data collection and structure refinement for structures **1** and **2** ($Sm_2Ga_{1.8}Ge_{5.2}$ and $Sm_4Ga_{5.24}Ge_{5.76}$) are given in Table 1. The atomic positions standardized with the STRUCTURE TIDY program [13] and atomic displacement parameters are listed in Table 2. The solid-solution boundaries for these two ternary phases were determined from the variation of their cell parameters in the full Ga/Ge concentration range. The cell parameters for $Sm_2Ga_{7-x}Ge_x$ and $Sm_4Ga_{11-x}Ge_x$ phases,
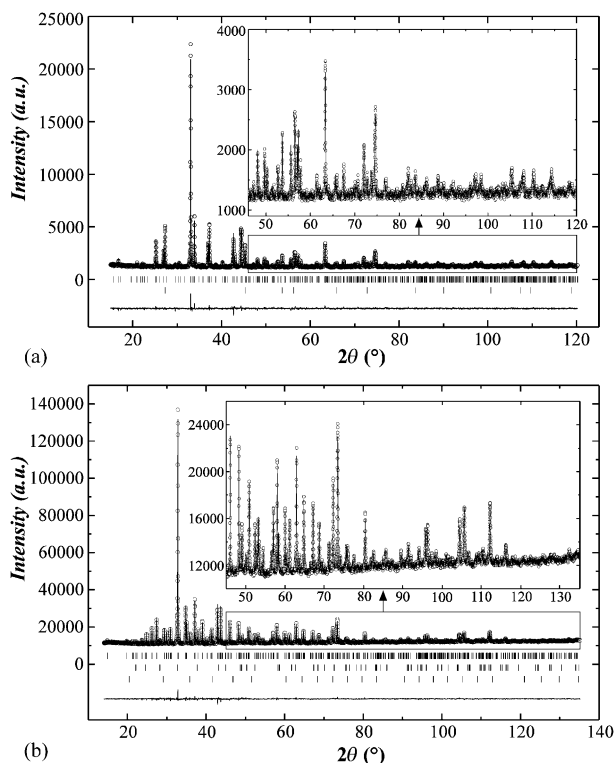
Fig. 1. Observed (circles), calculated (line) and difference (bottom line) X-ray powder diffraction patterns for $Sm_{22}Ga_{20}Ge_{58}$ (a) and $Sm_{28}Ga_{35}Ge_{37}$ (b) alloys. Vertical bars indicate the Bragg positions of contributing phases: $Sm_2Ga_{1.8}Ge_{5.2}$, 89.2(5) wt% and Ge, 10.83(9) wt% in (a); $Sm_4Ga_{5.24}Ge_{5.76}$, 98.0(3) wt%, $SmGa_{2-x}Ge_x$, 1.29(2) wt% and $SmGa_{3-x}Ge_x$, 0.70(1) wt% in (b).

Table 1
Crystal data and details of data collection and structure refinement for structures **1** and **2**

	$Sm_2Ga_{1.8}Ge_{5.2}$ (**1**)	$Sm_4Ga_{5.24}Ge_{5.76}$ (**2**)
Sample composition	$Sm_{22}Ga_{20}Ge_{58}$	$Sm_{28}Ga_{35}Ge_{37}$
$2\theta_{min-max}$ (deg.)	15–120.2	14–135.2
Step size, deg.; profile points	0.014432; 7289	0.014432; 8398
Number of "independent" and "effective" reflections	634; 352	500; 270
Number of refined structural parameters	21	20
Space group	Cmce (No. 64)	Cmmm (No. 65)
Pearson code, Z	oS80–8.00, 8	oS52–22.00, 2
Cell parameters:		
a (Å)	8.46216(13)	4.21038(4)
b (Å)	8.15343(13)	35.8075(3)
c (Å)	21.1243(3)	4.14023(4)
V (Å³)	1457.48(4)	624.193(9)
Preferred orientation: direction, value	[001], 0.897(2)	[010], 0.8935(11)
R_B	7.38	4.55
R_f	8.76	4.84
$R_p{}^a$	28.5, 2.54	16.9, 1.00
$R_{wp}{}^a$	16.5, 3.26	9.89, 1.35
χ^2	1.46	2.26

[a] Conventional and non-corrected for background.

Table 2
Atomic coordinates and isotropic displacement parameters in the $Sm_2Ga_{1.8}Ge_{5.2}$ and $Sm_4Ga_{5.24}Ge_{5.76}$ structures (X – Ga/Ge atoms)

Atom	Site	Occ.	x	y	z	U_{iso} (Å²)
$Sm_2Ga_{1.8}Ge_{5.2}$						
Sm	16g	1	0.2509(4)	0.3746(17)	0.08131(6)	0.0067(5)
X1	16g	1/2	0.0334(12)	0.1168(18)	0.1486(3)	0.0143(6)
X2	16g	1	0.2834(5)	0.1238(17)	0.19356(14)	0.0143(6)
X3	8f	1	0	0.114(3)	0.4618(3)	0.0143(6)
X4	8f	1	0	0.131(3)	0.0341(3)	0.0143(6)
X5	8f	1	0	0.3525(17)	0.3072(4)	0.0143(6)
X6	8f	1	0	0.4068(14)	0.1904(4)	0.0143(6)
$Sm_4Ga_{5.24}Ge_{5.76}$						
Sm1	4j	1	0	0.30079(2)	1/2	0.0048(5)
Sm2	4i	1	0	0.40041(2)	0	0.0046(5)
X1	16r	1/8	0.059(2)	0.06335(14)	0.438(2)	0.0024(9)
X2	8q	1/2	0.4265(10)	0.03363(7)	1/2	0.0024(9)
X3	8n	1/2	0	0.03308(6)	0.0711(11)	0.0024(9)
X4	4j	1	0	0.12750(7)	1/2	0.0257(13)
X5	4i	1	0	0.16660(6)	0	0.0033(9)
X6	4i	1	0	0.23248(6)	0	0.0015(9)

Table 3
Cell parameters for $Sm_2Ga_{7-x}Ge_x$ and $Sm_4Ga_{11-x}Ge_x$ phases

Ge (at%)	Lattice parameters (Å)			V (Å³)
	a	b	c	
$Sm_2Ga_{7-x}Ge_x$ ($x = 5.2{-}6.1$)				
53[a]	8.4619(2)	8.15267(19)	21.1242(6)	1457.30(8)
58	8.46216(13)	8.15343(13)	21.1243(3)	1457.48(4)
63	8.42729(19)	8.1097(2)	21.0532(5)	1438.83(6)
68	8.38432(16)	8.05936(16)	20.9809(4)	1417.73(5)
73[a]	8.3848(2)	8.05910(2)	20.9795(6)	1417.67(8)
$Sm_4Ga_{11-x}Ge_x$ ($x = 5.76{-}8.75$)				
33[a]	4.21095(7)	35.8111(5)	4.13955(7)	624.24(6)
37	4.21038(4)	35.8075(3)	4.14023(4)	624.193(9)
42	4.20911(5)	35.5544(2)	4.13851(5)	619.34(4)
47	4.20672(4)	35.2289(2)	4.13529(5)	612.84(4)
52	4.20476(5)	35.0091(2)	4.12593(5)	607.36(4)
57	4.20253(5)	34.81517(2)	4.11401(5)	601.93(4)
62[a]	4.20182(8)	34.81422(6)	4.11383(8)	601.78(7)

[a] Composition beyond the solid-solution boundaries.

determined respectively on five and seven alloys, are listed in Table 3.

3. Results and discussion

Interatomic distances and coordination numbers of atoms (CN) in their local environment are given in Table 4. The CNs of Sm atoms equal to 18 in **1** and 20 in **2**, and the coordination polyhedra made by the X atoms around Sm are very similar. Coordination polyhedra for Sm atoms in **2** are the same as those of the Th atom in the α-$ThSi_2$ structure. For both structures coordination polyhedron for the X1 atom is a tetragonal antiprism, with one square face capped by an X atom. The rest of X atoms have a trigonal-prismatic environment made of Sm and X atoms, with 2–3 X atoms capping side faces. The shortest Sm–X distances range 3.026(17)–3.300(3) Å in **1** and

Table 4
Interatomic distances (d) and coordination numbers of atoms (CN) in the $Sm_2Ga_{1.8}Ge_{5.2}$ and $Sm_4Ga_{5.24}Ge_{5.76}$ structures (X – Ga/Ge atoms)

$Sm_2Ga_{1.8}Ge_{5.2}$			$Sm_4Ga_{5.24}Ge_{5.76}$		
Atoms	d (Å)	CN	Atoms	d (Å)	CN
Sm–12X	3.026(17)–3.300(3)	18	Sm1–12X	3.1750(9)–3.321(2)	20
Sm–6Sm	3.991(10)–4.246(5)		Sm1–8Sm	4.124(2)–4.210(2)	
X1–2X2	2.320(11)	9	Sm2–14X	3.1169(9)–3.248(10)	20
X1–X5	2.366(19)		Sm2–6Sm	4.140(2)–4.210(2)	
X1–X4	2.438(9)		X1–2X3	2.316(10), 2.384(10)	9
X1–X6	2.540(18)		X1–2X2	2.317(10), 2.429(10)	
X1–4Sm	3.042(15)–3.496(15)		X1–1X4	2.324(6)	
X2–X1	2.320(11)	8	X1–4Sm2	3.242(10)–3.248(10)	
X2–X2	2.451(4)		X2–2X1	2.317(10), 2.429(10)	9
X2–X6	2.549(13)		X2–1X2	2.408(4), 2.487(4)	
X2–X5	2.615(15)		X2–4X3	2.526(4)	
X2–X5	3.263(14)		X2–2Sm2	3.156(2)	
X2–X6	3.329(13)		X3–2X1	2.316(10), 2.384(10)	9
X2–2Sm	3.136(13)–3.143(13)		X3–2X3	2.369(3), 2.441(4)	
X3–X3	2.466(19)	8	X3–4X2	2.526(4)	
X3–X4	2.575(19)		X3–2Sm2	3.192(2)	
X3–6Sm	3.026(17)–3.300(6)		X4–1X1	2.324(6)	9
X4–X1	2.438(9)	9	X4–2X5	2.499(2)	
X4–X3	2.575(19)		X4–6Sm	3.1169(9)–3.321(2)	
X4–X4	2.581(19)		X5–1X6	2.359(3)	9
X4–6Sm	3.071(17)–3.223(6)		X5–2X4	2.499(2)	
X5–X1	2.366(19)	8	X5–6Sm	3.1750(9)–3.1919(19)	
X5–X6	2.506(12)		X6–1X5	2.359(3)	9
X5–2X2	2.615(15)		X6–2X6	2.4508(17)	
X5–2Sm	3.166(7)		X6–6Sm1	3.1837(9)–3.2045(19)	
X5–2X2	3.262(14)				
X6–X5	2.506(12)	8			
X6–X1	2.540(18)				
X6–2X2	2.549(13)				
X6–2Sm	3.145(6)				
X6–2X2	3.329(13)				

3.1170(9)–3.471(12) Å in **2**, slightly exceeding a sum of atomic radii ($r_{Sm} = 1.802$ Å, $r_{Ga} = 1.221$ Å and $r_{Ge} = 1.225$ Å [14]).

Pseudo-tetragonal structures **1** and **2** are shown in Fig. 2, with highlighted three-dimensional X-atom frameworks. The most striking feature in these structures is the X_8 empty cubes capped by X1 atoms. In **1** the cubes are ordered, with one face enlarged due to the bridging function of the X1 atom. This face is not perfectly square but rather rhomb-like, the lengths of the two diagonals differing by ~0.3 Å. The X1 atom is disordered along the longer diagonal of this face, tending to achieve a four-bonded state instead of a five-bonded one in an idealized ordered structure. Disorder is more pronounced in **2**, where the whole fragment, consisting of the distorted X_8 cube capped by the X1 atom, is disordered. This results in the apparent splitting of the additional X positions (X2 and X3), however, the average structure of **2** can be interpreted by the same local atomic arrangement as in **1** (see Fig. 2). Similar fragments have been found in other Ga- and Ge-rich intermetallic compounds. For example, $RE_2Zn_3Ge_6$ (RE = La, Ce, Pr, Nd) structures [15] contain the same distorted cubes of Ge atoms, each capped on one face by Zn atom (Fig. 3c). As compared to structure **1** (Fig. 3a), the

cube in $RE_2Zn_3Ge_6$ differs only by its Zn-capped face, which appears to be practically an ideal square. Consequently, the Zn atom was found to be ordered. Ga-based cubes discovered in the structure of $YbGa_5$ [4] differ more distinctly. Not one, but two opposite faces of the Ga_8 cube are capped by additional Ga atoms. The main difference, however, concerns the direction of the disorder in the Ga_8 cube (compare Figs. 3b and d). It was suggested [4] that the disorder in the Ga_{8+2} cage is induced by a tendency of three-bonded Ga atoms, located in the corners of the Ga_8 cubes, to achieve the "optimum" distances and a four-bonded state. These Ga atoms are split in the direction perpendicular to the direction of the atomic disorder in **2** (Fig. 3b). Gallium atoms in a five-bonded state (those that cap two opposite faces) tend to compensate the distortion of the cube, resulting in a peculiar disorder pattern for the whole fragment (Fig. 3d). A fully ordered undistorted Ga_8 cube was found in the closely related structures of $YCoGa_3Ge$ and $YNiGa_3Ge$ [16] (similar to $YbGa_5$, they are defect variants of $Ce_2Ga_{10}Ni$ [17]). These isostructural quaternary compounds, studied both by X-ray and neutron single-crystal diffraction, reveal an ordered arrangement of Ga and Ge atoms. Two opposite faces of the Ga_8 cubes are capped by Ge atoms, which, unlike all other examples, are
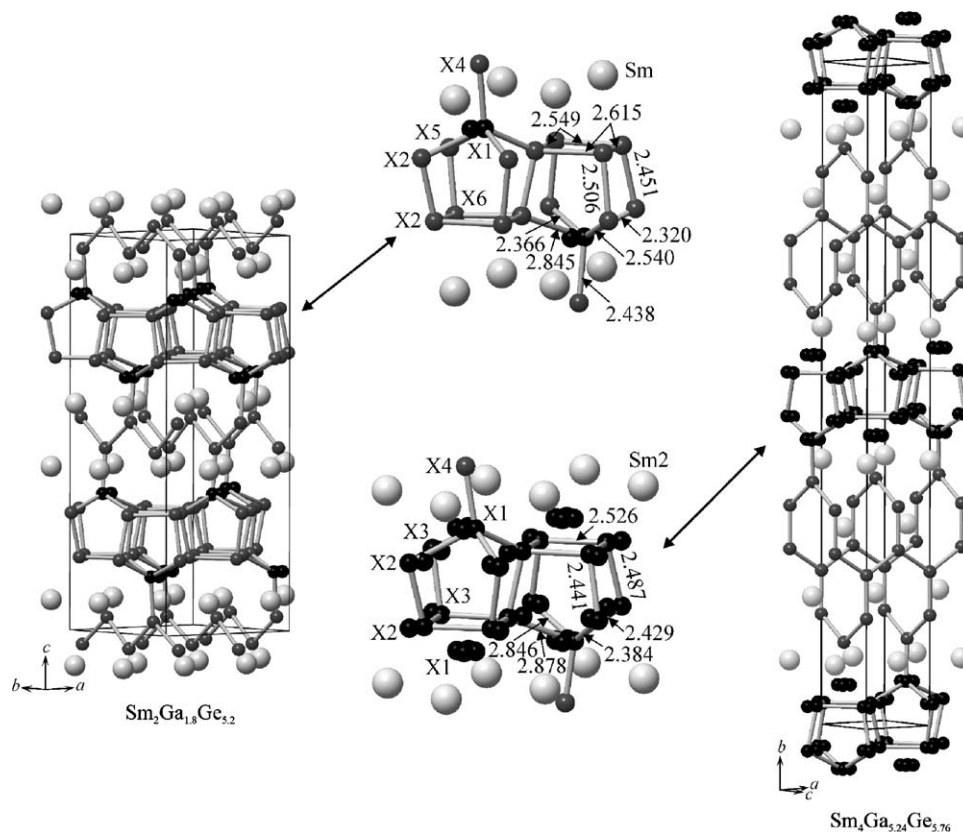
Fig. 2. $Sm_2Ga_{1.8}Ge_{5.2}$ (1) and $Sm_4Ga_{5.24}Ge_{5.76}$ (2) structures containing three-dimentional frameworks of X atoms. Atoms in split positions are shown by black spheres. In 1 distorted X_8 cubes are capped on one side by an atom in the split $X1$ position. An apparent disorder in 2 can be interpreted by the same local atomic arrangement.
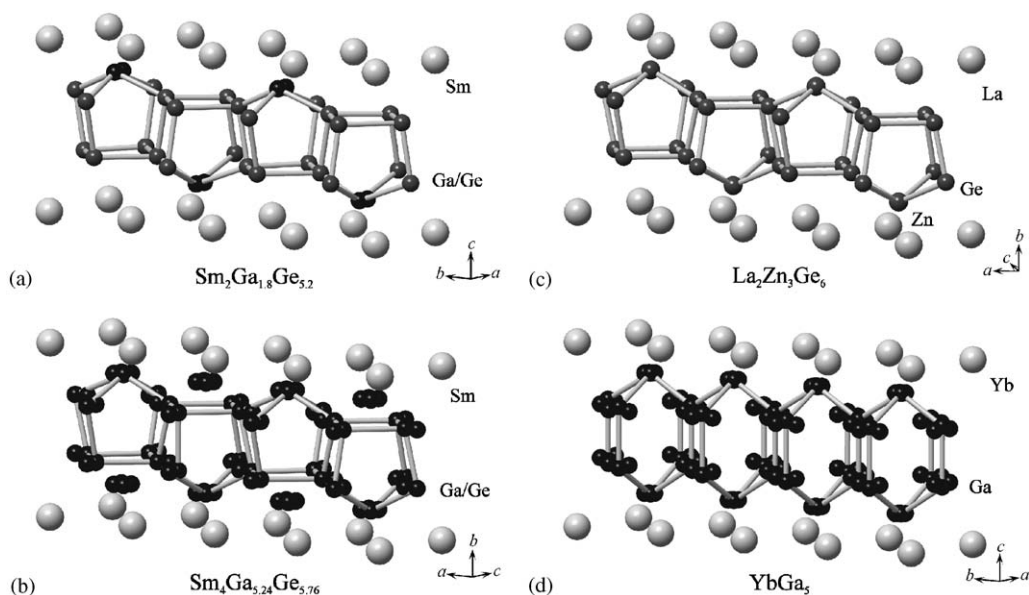
Fig. 3. Empty Ga/Ge cubes capped by additional atoms in the structures of $Sm_2Ga_{1.8}Ge_{5.2}$ (a), $Sm_4Ga_{5.24}Ge_{5.76}$ (b), $La_2Zn_3Ge_6$ (c) and $YbGa_5$ (d). Atoms in split positions are shown by black spheres.

disordered in the direction perpendicular to the capped face (not shown in Fig. 3). The above structure comparisons and a relatively low Ga content in 1 and 2 suggest that the X_8 cubes in the title structures are predominantly formed by Ge atoms, while the $X1$ positions are presumably rich in Ga. The Ga-poor structure 1 is very similar to the Ge-based $RE_2Zn_3Ge_6$ (compare Figs. 3a and c), while the relatively Ga-rich structure 2 contains very disordered

structural units, which are comparable to, though notably different from, those in $YbGa_5$.

The structures **1** and **2** are closely related not only with respect to the geometry of the X_8 cubes. The structures can be described in terms of linear intergrowth of segments of the $BaAl_4$, AlB_2 and α-Po structure types [18,19]. The $BaAl_4$ segment is built up by an empty and $X1$-centred tetragonal antiprisms, alternating along ab (**1**) and ac (**2**). The AlB_2 layer consists of trigonal prisms of Sm atoms centred by X atoms. The structure **1** contains only one AlB_2 layer, while the structure **2** contains three AlB_2 layers, mutually rotated by 90° (such an arrangement can be described alternatively as the α-$ThSi_2$ structure blocks). The α-Po segment consists of empty X_8 cubes, each of which is composed from two Ga_4 square faces of the neighbouring $BaAl_4$ blocks. The intergrowth of the three types of segments in the structures **1** and **2** is shown in Fig. 4. An intergrowth of the $BaAl_4$, AlB_2 and α-Po fragments has also been established [19] in $SmNiGe_3$ [9] and La_2AlGe_6 [20] structure types. The orthorhombic structure **1** ($Ce_2(Ga_{0.1}Ge_{0.9})_7$ structure type) and the monoclinic La_2AlGe_6 are vacancy-ordering variants of

the $SmNiGe_3$ structure type. For both structures the vacancy ordering in the $BaAl_4$-type segments results in doubling of the two shortest translation periods, as compared to $SmNiGe_3$ (see Fig. 4). It is worth to note, that in the Y–Ga–Ge system all three types of structure, namely $Ce_2(Ga_{0.1}Ge_{0.9})_7$, $SmNiGe_3$ and La_2AlGe_6, exist at the same temperature (600 °C) [21]. The closely related $YbGa_5$ and $Ce_3Ni_2Si_8$ [22] structures contain only two types of segments (Fig. 4). The latter is built up from segments of $BaAl_4$ and AlB_2, but not of $BaAl_4$ and α-$ThSi_2$ as reported earlier [22]. The structures **1** and **2** are very similar so far as they belong to the same structure series and are built up from the same structural blocks. Both structures contain X_8 cubes caped on one side by an X atom. In contrast to the disordered structure **2,** an ordered arrangement of the X_{8+1} assemblies in **1** results in doubling of the two shortest translation periods.

Ternary compounds of general formula $RE_2Ga_{7-x}Ge_x$ and $RE_4Ga_{11-x}Ge_x$ (RE = rare earth atom) were found in other RE–Ga–Ge systems [5,23,24]. The $Ce_2(Ga_{0.1}Ge_{0.9})_7$ structure type has been assigned to all $RE_2Ga_{7-x}Ge_x$ phases, but the structure was determined only for R = Ce
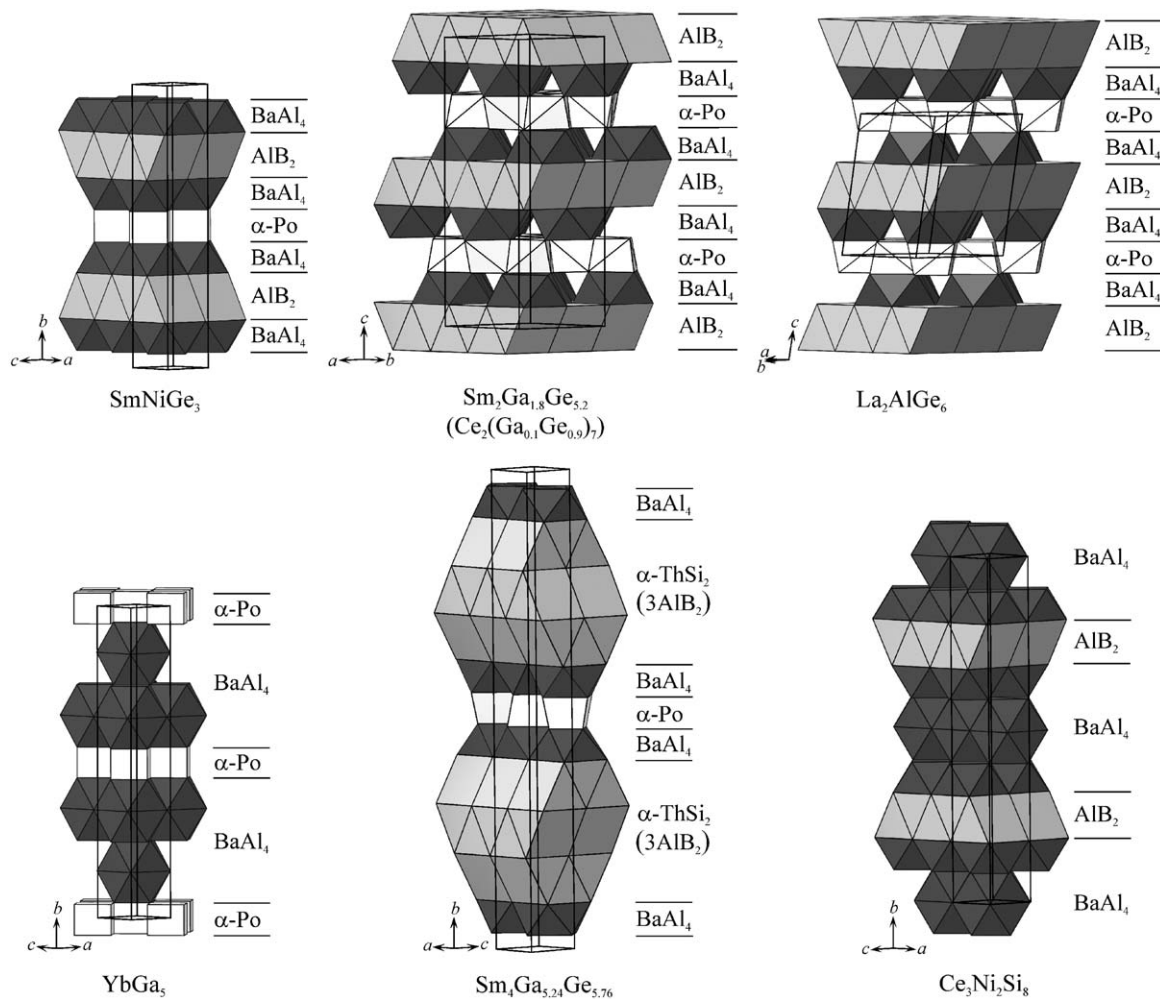
Fig. 4. $SmNiGe_3$, $Ce_2(Ga_{0.1}Ge_{0.9})_7$, La_2AlGe_6 and $Sm_4Ga_{5.24}Ge_{5.76}$ structure types presented as a linear structure series, composed of $BaAl_4$, AlB_2 and α-Po structure segments. $YbGa_5$ and $Ce_3Ni_2Si_8$ structures contain only two types of segments.

and Tb [8,24]. However, disorder of the $X1$ position in this type of structure was identified in the present article for the very first time. The crystal structures of the $R_4Ga_{11-x}Ge_x$ compounds were not determined before, but an orthorhombic $La_4Ga_4Ge_7$ structure type was mentioned [5] without any reference. For that reason we have measured X-ray diffraction patterns for three $RE_4Ga_{11-x}Ge_x$ compounds ($RE = $ La, Pr and Nd) and compared them with the data on **2**. Their similarity suggests that the $RE_4Ga_{11-x}Ge_x$ structures belong to the $Sm_4Ga_{5.24}Ge_{5.76}$ structure type.

Finally, we want to draw attention to the variation of the unit cell volume as a function of Ga/Ge ratio. The scan over the range of solid solutions for $Sm_2Ga_{7-x}Ge_x$ and $Sm_4Ga_{11-x}Ge_x$ shows (see Table 3), that the cells are noticeably contracted when Ga atoms are replaced by Ge. These changes cannot be explained by size factors because of the very similar radii of Ga and Ge atoms ($r_{Ga} = 1.221$ Å and $r_{Ge} = 1.225$ Å [14]). The contraction is practically isotropic for $Sm_2Ga_{7-x}Ge_x$: in the whole concentration range the pseudo-tetragonal cell is contracted by ~1.0% in the basal plane and by ~0.7% along the c axis. However, contraction is highly anisotropic for $Sm_4Ga_{11-x}Ge_x$: by only ~0.4% in the basal plane and by over 2.8% perpendicular to it (along the b axis). Considering the strong similarity of the structures **1** and **2**, this difference can only be attributed to a threefold increase in the amount of AlB_2 segments in the structure **2**. Such an explanation is coherent with the behaviour of the α-$ThSi_2$-type ternary in the Sm–Ga–Ge system. The unit cell of the $SmGe_{1.4-1.1}Ga_{0.6-0.9}$ solid solution contracts anisotropically when Ga atoms are replaced by Ge: the cell shrinks by 0.14% in the basal plane and by 0.48% along the c axis [12], very much as in **2**. This observation was explained by stronger covalent interactions X–X at compositions rich in Ge [12]. The assumption that Ga substitutes Ge primarily in the α-$ThSi_2$ (or AlB_2) blocks is highly consistent with lower Ga content in **1** ($Sm_2Ga_{7-x}Ge_x$) than in **2** ($Sm_4Ga_{11-x}Ge_x$): 10–20% in the former versus 15–35% in the latter.

In view of the above considerations we suggest the following model of the Ga/Ge localization in $Sm_2Ga_{7-x}Ge_x$ and $Sm_4Ga_{11-x}Ge_x$. The X_8 cubes are formed by Ge atoms, while the Ga-rich $X1$ positions stabilize the X_{8+1} fragment, providing formation of the ternary compounds very much in the same way as Zn, Ni and Al atoms do in $RE_2Zn_3Ge_6$, $SmNiGe_3$ and La_2AlGe_6. The partial replacement of Ge atoms by Ga within the solid solutions takes place primarily in the AlB_2 and α-$ThSi_2$ structure blocks.

4. Conclusions

New ternary compounds $Sm_2Ga_{7-x}Ge_x$ ($x = 5.2-6.1$) and $Sm_4Ga_{11-x}Ge_x$ ($x = 5.76-8.75$) were synthesized and their crystal structures were determined by X-ray powder diffraction at compositions $Sm_2Ga_{1.8}Ge_{5.2}$ and $Sm_4Ga_{5.24}Ge_{5.76}$. The former crystallizes with the $Ce_2(Ga_{0.1}Ge_{0.9})_7$ structure, the latter with its own type of

structure. Both structures are members of the linear intergrowth structure series built up from segments of $BaAl_4$, AlB_2 (or α-$ThSi_2$) and α-Po structure types. Their Ga/Ge networks contain characteristic empty cubes with one side capped by an X atom subjected to an intrinsic displacive disorder. An ordered arrangement of the X_{8+1} assemblies in $Sm_2Ga_{7-x}Ge_x$ results in doubling of the two shortest cell translation periods, as compared to the structure $Sm_4Ga_{11-x}Ge_x$. Although Ga and Ge atoms were not distinguished by X-ray diffraction, the following model of Ga/Ge localization was suggested on the basis of crystal-chemical analysis. The X_8 cubes are formed by Ge atoms, while the Ga-rich positions capping the cubes stabilize the X_{8+1} fragment. A partial replacement of Ge atoms by Ga within the solid solutions takes place in the AlB_2 and α-$ThSi_2$ structure blocks.

References

[1] Yu. Grin', R.E. Gladyshevskii, Gallides. Handbook, Metallurgia, Moscow, 1989 (in Russian).
[2] G. Bruzzone, M.L. Fornasini, F. Merlo, J. Less-Common Met. 154 (1989) 67–77.
[3] F.H. Ellinger, W.H. Zachariasen, Acta Crystallogr. 19 (1965) 281–283.
[4] R. Giedigkeit, R. Niewa, W. Schnelle, Yu. Grin, R. Kniep, Z. Anorg. Allg. Chem. 628 (2002) 1692–1696.
[5] Red Book. Constitutional Data and Phase Diagrams of Metallic Systems. Year 1996, MSI GmbH 41, 1999.
[6] M.G. Kanatzidis, R. Pöttgen, W. Jeitschko, Angew. Chem. Int. Ed. 44 (2005) 6996–7023.
[7] J. Rodriguez-Carvajal, FULLPROF SUITE, LLB Sacley and LCSIM Rennes, France, 2003.
[8] Ya.P. Yarmolyuk, V.K. Pecharskii, I.A. Gryniv, O.I. Bodak, V.E. Zavodnik, Sov. Phys. Crystallogr. 34 (1989) 174–176.
[9] O.I. Bodak, V.K. Pecharskii, O.Ya. Mruz, V.Yu. Zavodnik, G.M. Vitvitskaya, P.S. Salamakha, Dopov. Akad. Nauk Ukr. RSR Ser. B. (1985) 36–38.
[10] A. Boultif, D. Louër, J. Appl. Crystallogr. 24 (1991) 987–993.
[11] V. Favre-Nicolin, R. Černý, J. Appl. Crystallogr. 35 (2002) 734–743.
[12] Ya. Tokaychuk, Ph.D. Thesis, University of Lviv, 2005.
[13] L.M. Gelato, E. Parthé, J. Appl. Crystallogr. 20 (1987) 139–143.
[14] J. Emsley, The Elements, Oxford University Press, Oxford, 1997.
[15] J.R. Salvador, D. Bilc, J.R. Gour, S.D. Mahanti, M.G. Kanatzidis, Inorg. Chem. 44 (2005) 8670–8679.
[16] M.A. Zhuravleva, R.J. Pcionek, X. Wang, A.J. Schultz, M.G. Kanatzidis, Inorg. Chem. 42 (2003) 6412–6464.
[17] Ya.P. Yarmolyuk, Yu.N. Grin, I.V. Rozhdestvenskaya, O.A. Usov, A.M. Kuz'min, V.A. Bruskov, E.I. Gladyshevskii, Sov. Phys. Crystallogr. 27 (1982) 599–600.
[18] Yu.N. Grin', Ya.P. Yarmolyuk, E.I. Gladyshevskii, Sov. Phys. Crystallogr. 27 (1982) 413–417.
[19] Yu.N. Grin', in: E. Parthé (Ed.), Modern Perspectives in Inorganic chemistry, NATO ASI Series, Series C: Math. Phys. Sci., vol. 382, 1992, pp. 77–95.
[20] J.T. Zhao, K. Cenzual, E. Parthé, Acta Crystallogr. C 47 (1991) 1777–1781.
[21] M.V. Speka, M.I. Zhakharenko, V.Ya. Markiv, N.M. Belyavina, J. Alloy Compd. 367 (2004) 41–46.
[22] V. Fritsch, S. Bobev, J.D. Thompson, J.L. Sarrao, J. Alloy Compd. 388 (2005) 28–33.
[23] Yu.N. Grin, P. Rogl, B. Chevalier, A.A. Fedorchuk, I.A. Gryniv, J. Less-Common Met. 167 (1991) 365–371.
[24] A.O. Fedorchuk, T.V. Dol'nikova, in: Abstracts of the XIV Ukraine Conference on Inorganic Chemistry, September 10–12, 1996, p. 179.